Automated Analysis of Rodent Three-Channel Electrocardiograms and Vectorcardiograms

HUNG T. LE, WILLIAM C. VAN ARSDEL, ARMAND M. MAKOWSKI, MEMBER, IEEE, ERIK W. POTTALA, AND JAMES J. BAILEY

Abstract—Exposure to toxic substances often produces alterations in heart rhythm and electrocardiographic waveform parameters such as *PR* interval, *ST*, etc. Analysis of such physiological changes is believed to provide sensitive indicators for revealing the degree of toxicity sustained. The purpose of this paper is to describe a system for automated analysis of electro- and vectorcardiograms in cardiotoxicity studies on rats. A selection of the best-suited methods of digital signal processing is also described.

I. Introduction

INVESTIGATORS have been using rodent electrocardiograms (ECG) to monitor cardiotoxicity for 50 years [1]. Because the rodent is an inexpensive model for testing, the rodent ECG has been used increasingly by the pharmaceutical industry and agencies such as the Food and Drug Administration for acute and chronic toxicity trials, nutritional studies, and testing of food additives and drugs [2].

Up until recently, the standard practice in the pharmaceutical industry was to use a manually read, single-lead ECG and to define premature or ectopic beats as an end point for toxicity [3]. This practice is believed to be insufficient in determining the level of toxicity since changes in conduction, depolarization, and repolarization patterns can reveal a level of toxicity at a much earlier stage.

In the past, rodent ECG's have been recorded on a human ECG chart. Due to the inappropriate frequency response (100 Hz cutoff) of the amplifiers and recording devices, true changes as reflected by the *QRS-T* patterns, *P-R* interval, etc., may not be determined since rodent ECG's contain frequencies which are much higher than 100 Hz. In addition, a single-lead ECG may not reveal the correct onsets and offsets (fiducials) of waves and/or the changes in wave patterns owing to dipole vector forces which are orthogonal to the lead vector. No single-channel chart can therefore provide the opportunity to construct three-space vector loops or vectorcardiograms (VCG). These vector loops can show changes in morphology which are often not clearly apparent in the single ECG trace; this is why VCG's are often done as a complementary study to the routine ECG in humans.

Another basic difficulty in the ECG/VCG analysis is created by power line interference, random muscle noise, and baseline wander, which can severely affect the determination of fiducials and pattern changes. Analog methods are not well suited for dealing with this problem, and in the case of muscle noise, they are completely inadequate. On the other hand, digital processing of the signal can enhance the signal-to-noise ratio (SNR) and minimize the effect of these disturbances, thereby improving the reliability of determining fiducials and true pattern alterations.

Therefore, it would appear that a well-designed system for automated ECG analysis could produce more accurate and more sensitive indicators for cardiotoxicity, while at the same time saving a great deal of manpower and money. Such a system would be of great benefit to investigators interested in testing cardiotoxicity of drugs or animal models of cardiac disease. In addition, the ability to rapidly analyze rodent ECG's with great accuracy further encourages the use of a greater number of animals per study, thereby improving the overall statistical power of such studies.

The purpose of this paper is to describe a new system, which has been successfully implemented at the Laboratory of Applied Studies, for the automated analysis of rodent ECG's in toxicological studies. A selection of the best suited of digital signal processings is illustrated; this includes analog and digital filtering, baseline removal using cubic spline fitting, and signal averaging. In addition, the methods employed to determine fiducials result in reasonable and reproducible demarcation of atrial activity, ventricular depolarization, and ventricular repolarization to the extent to which they can be separately identified in the surface ECG.

II. Data Collection System: Description

In this section, analog recordings, hardware system, analog-to-digital conversion, and signal storage are described.

A. ECG Recordings

Rat ECG's are recorded on a seven-track analog tape recorder at a speed of $3\frac{3}{4}$ in/s. The front end of the recorder consists of an amplifier with a frequency response from 0 to 1500 Hz.

Four simultaneous channels, namely, leads I, AVF, SAVF, and II, are recorded on tape, with the fifth channel reserved for event code (rat number, reading time in hours, minutes, and seconds). At the end of each rat ECG record (1-2 min in duration), a calibration pulse of 1 mV is inscribed on all four channels.

Manuscript received December 8, 1983; revised October 1, 1984.

H. T. Le was with the Laboratory of Applied Studies, Division of Computer Research and Technology, National Institutes of Health, Bethesda, MD 20205. He is now with the IBM Corporation, Manassas, VA 22110.

W. C. Van Arsdel is with the Division of Drug Biology, Center for Drugs and Biologics, Food and Drug Administration, Washington, DC 20204.

A. M. Makowski is with the Department of Electrical Engineering, University of Maryland, College Park, MD 20740.

E. W. Pottala and J. J. Bailey are with the Medical Applications Section, Laboratory of Applied Studies, Division of Computer Research and Technology, National Institutes of Health, Bethesda, MD 20205.

U.S. Government work not protected by U.S. copyright

B. Hardware System

The system consists of a MAC-16 multiprogramming computer, equipped with a nine-track digital magnetic tape, an eight-channel analog-to-digital converter, an ARDS graphic display/keyboard, and an ASR-33 teletype.

In addition, a Honeywell system, consisting of an analog tape recorder/reproducer, a Systron/Donner time code reader/generator, and a Systron/Donner tape search unit, is used for playing prerecorded ECG tapes during analog-to-digital conversion.

C. ADC and Signal Storage

Analog-to-digital conversion (ADC) is performed off line on the MAC-16 which contains a 12-bit A/D converter and eight sample and hold circuits for simultaneous data samples. Operation of the ADC system consists of initializing the multiplexed data channel with address, block size, etc., and of issuing a command word to the real-time clock to select the sampling rate. To reduce high-frequency noise and aliasing (Nyquist rate), hardware filtering is performed with a programmable switch/filter before the A/D conversion. The low-pass filters are all six-pole Butterworth filters.

Data values from the A/D process are stored as 16-bit integers in three alternating buffers, with a size of 2400 words (800 words/channel). Once a buffer is filled with data, it will be transferred onto the digital mag tape. In one A/D conversion, 22 400 data values are collected on tape for each animal.

Once the A/D process is completed, the data are than read and stored on disk for processing on an IBM 360/370 machine.

III. Signal Analysis

As indicated earlier, the rat data were recorded on analog tape at a speed of $3\frac{3}{4}$ in/s. These data are reproduced from a tape drive at half the recording speed and are digitized at 1250 Hz. This results in an effective sampling rate of 2500 Hz. To avoid interference and information losses (aliasing), the analog data are passed through a 500 Hz Butterworth low-pass filter with an effective cutoff frequency of 1000 Hz. Note that the sampling rate is slightly higher than twice the highest frequency component of the signal to allow for a nonperfect filter characteristic.

A. Preprocessing

The presence of noise/interference in the recorded electrocardiograms can create large deviations from the true amplitude and phase characteristics of the ECG signal. Among these interference sources, it is useful to distinguish

1) baseline drift caused by rodent movement or imperfect electrode contact,

2) muscle potential spikes which accompany body movements or muscle tremor,

3) power line interference which causes periodic high-frequency alterations of the baseline,

4) periodic low-frequency alteration of the baseline caused by respiration.

Preprocessing is crucial to reduce interference on the ECG signal by minimizing the above sources of noise and artifacts. Hence, the signals are subjected to the following preprocessing steps to allow for a precise parameter and feature extraction. For a complete illustration, see Fig. 1.

1) Digital Filtering: A spectral analysis of the rat ECG's indicates that it is band limited between 0 and 200 Hz. Any frequency component in the ECG above 200 Hz is at least 30 dB down from the peak spectral component.

In the removal of high-frequency noise, the digitized data are filtered with a low-pass windowed finite-impulse response (FIR) having a 200 Hz cutoff frequency (see Fig. 2). This filtering process [4] is also known as moving average since each sampled value of the ECG is replaced by a weighted combination of the values at several adjacent sampling points, thus reducing the effect of random variations at any one data point. Such filters are often implemented because of their precise linear phase characteristic; this is crucial here since the ECG signals must be in a linear time phase relationship to each other. Indeed, implementation of a nonlinear phase filter would cause gross distortions to the ECG waveforms. In addition, nonrecursive FIR filters are inherently stable, conceptually simple to design, and are relatively insensitive to the effects of quantization error [4].

2) Baseline-Drift Determination, Evaluation, and Correction

a) Baseline Definition: There is some controversy as to where to establish the baseline reference, the so-called "isoelectric baseline." However, the best choice for a reference level seems to be the point immediately before the *QRS* complex (*P-R* knots) since the least amount of error in baseline alterations is encountered here [5]. The reader is referred to Section III-B1) for a method of *QRS*-onset detection [see Fig. 1(a)].

b) Baseline Evaluation and Correction: Computer processing of electrocardiograms requires the ECG signal to have a reasonably steady baseline since measurements of wave amplitude are made relative to the baseline. Thus, any baseline drift resulting from rodent movements or respiration must be reduced.

For low-frequency baseline wander, high-pass filtering can be used; however, attempts to filter out higher frequency baseline drifts would unfortunately attenuate the lower band frequency of the signal.

The method outlined below uses a regression on a set of fiducial points (*P-R* knots) in each individual channel by using a polynomial of order three or cubic spline which estimates the respiratory artifacts [6]. The third-order fitting polynomial is chosen over a higher order polynomial for ease of implementation since fewer constants need to be evaluated. In addition, the power spectral density of the cubic spline interpolators closely approximates the band-limited white noise spectrum [7]. Simple calculations showed that implementation of a fifth-order polynomial approximation would only improve the frequency response by an approximate 0.5 dB, while the number of constants to be evaluated would quadruple from three constants in the cubic case to twelve in the quintic case.

While the above process removes higher frequency baseline noise, it also preserves low-frequency heart information. Furthermore, such a method can also be used effectively to remove the respiratory artifacts (heart-rate dependent) since the set of *P-R* knots residing on the spline function is also directly related to the heart rate. In effect, a "self-adjustable" high-pass filter is being implemented.

The baseline removal process consists of estimating the baseline drift by fitting a third-order polynomial through a set of

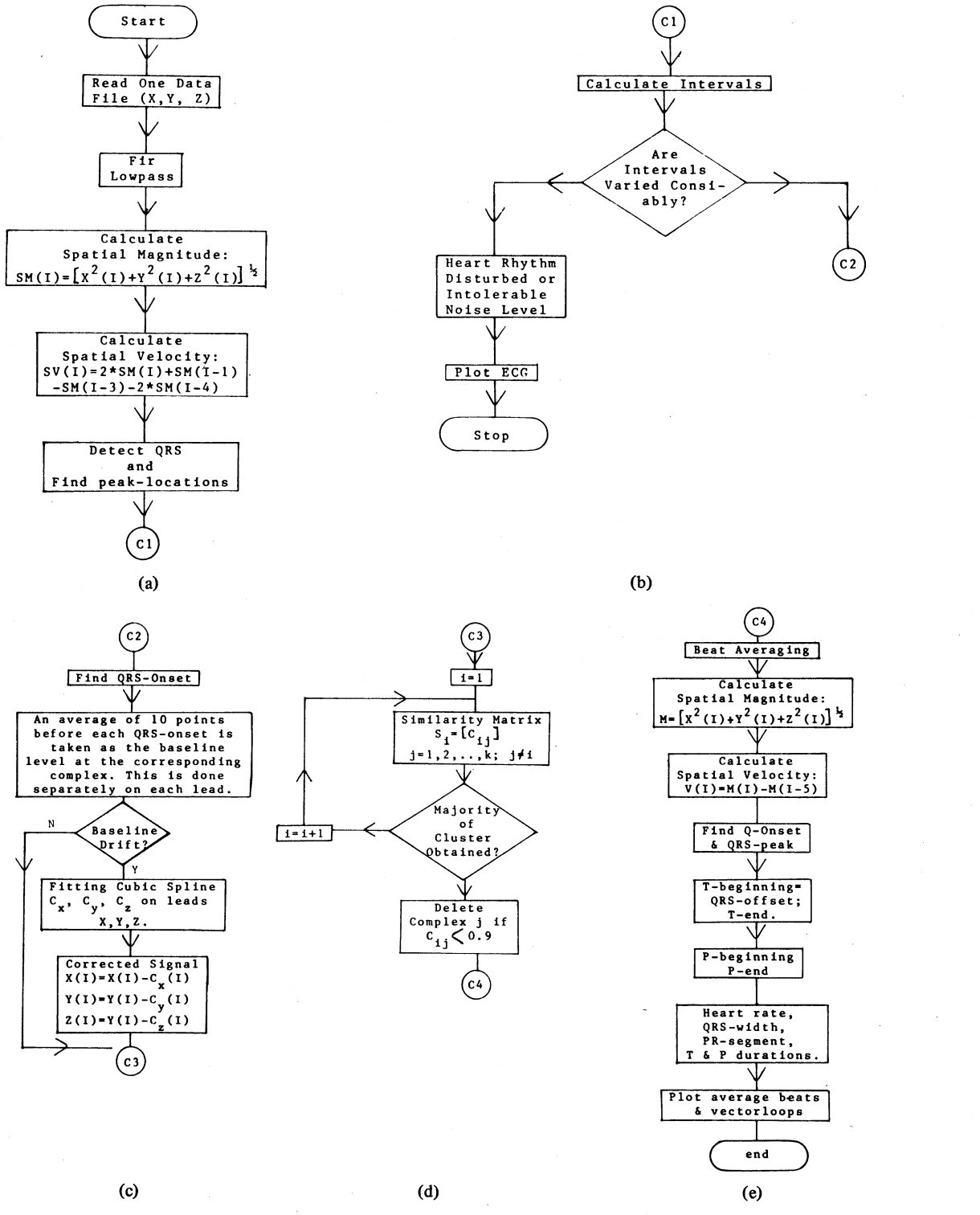

Fig. 1. Program flowchart.

predetermined fiducial points (*P-R* knots), and then subtracting the noise estimate from the original ECG signal. The results of baseline noise removal are illustrated in Fig. 3.

3) Template Formation: The extraction of parameters from individual beats is still rather difficult, if not impossible, since much of the ECG signal is still corrupted by noise/interference. Furthermore, computer analysis of such a low-quality ECG signal could result in unreliable parameter measurements. To further improve the signal quality (signal-to-noise ratio), signal averaging can be used, assuming that the corrupting noise is random [8]. Since the ECG waveforms are periodic, an average beat can be formed by summing over a number of heart cycles. In order to obtain a "representative" beat from signal averaging, ventricular premature beat or artifacts must be removed from the averaging process.

To differentiate the abnormal beats from the normal ones, a similarity matrix S_i of dimension $1 \times (K-2)$ is introduced, $(K-1)$ being the number of heart cycles and K being the number of R peaks available, with

$$S_i = [C_{ij}], \quad j = 1, 2, \ldots, K-1; \quad i \neq j$$
$$i = 1, 2, \ldots, K-1$$

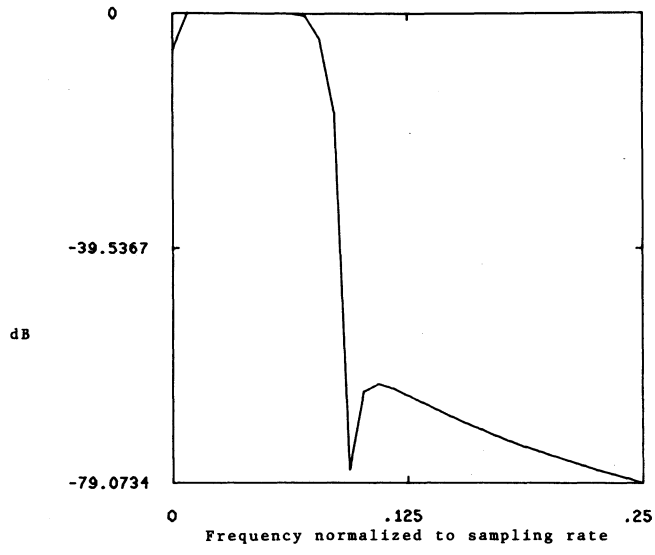

Fig. 2. Frequency response to FIR filter (Hamming window).

and C_{ij}'s are the cross-correlation coefficients between complexes i and j. If complex i, where $i = 1$, is not a "representative" or normal beat, the next complex, i.e., $i = 2$, will be chosen as a reference beat. This procedure is iterated until a majority cluster of similar complexes is obtained. Any complex which yields a cross-correlation coefficient less than 0.90 is then deleted from the data set. The reader is referred to Fig. 1(d).

4) Beat Averaging: Signal averaging can be used to further improve the signal-to-noise ratio by summing over a number of consecutive periods. Since noise is assumed to be random [5], [8], the noncoherent noise is added out of phase, and therefore tends to decrease with each addition, while the coherent portions of the input ECG signal reinforce each other with each successive addition. Fig. 4 illustrates the noise suppression in the time and frequency domain by using signal averaging. In this figure, the residuals were obtained by subtracting the 14th average (i.e., average of 14 complexes) from the corresponding (lesser) averages.

The averaging process is performed as follows.

If K is the number of R peaks available within one file of data (5600 points/ECG lead), then there exist $(K - 1)$ heart cycles; here, a heart cycle is defined as the number of samples from one peak to the next.

Before any averaging can be performed, individual heartbeats must be properly aligned. To achieve this, critical values within the complexes, namely, the R peaks, must be used as synchronization points. However, due to heart rate variations, the number of samples N_j within complex j may be different from any other complex ($j = 1, 2, \cdots, K - 1$). Therefore, elimination of a number of samples which lie within the inactive region (namely, the T-P interval) is required. The choice of such a procedure is based on the fact that small variations in the heart rate only affect the segment between the T wave and the P wave [1].

Once all beats are properly aligned with an equal number N of sample values within any one complex (i.e., $N = N_j$, $j = 1, 2, \cdots, K - 1$), averaging can be computed by the following

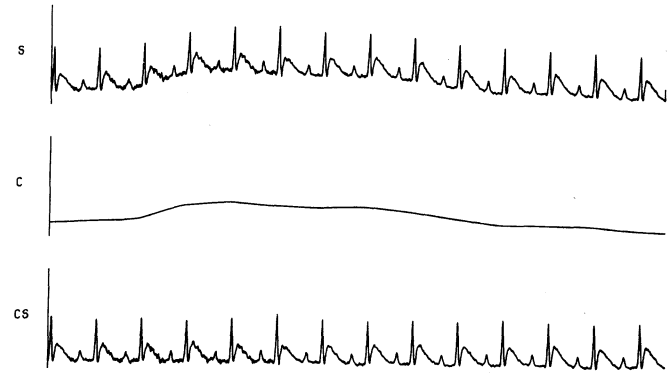

Fig. 3. Baseline correction using cubic splines; S represents the raw data. C represents the baseline estimates. CS represents the corrected signal ($CS = S - C$).

equation:

$$y_i = \frac{1}{K-1} \sum_{j=1}^{K-1} y_{ij}$$

where y_i represents the ECG amplitude measured at time $t = i$ ($i = 1, 2, \cdots, N$), and y_{ij} indicates the ECG amplitude measured at time $t = i$ of complex j ($i = 1, \cdots, N$ and $j = 1, \cdots, K - 1$).

A more efficient algorithm can be obtained as follows.

Let M_j ($j = 1, \cdots, K$) represent the peak locations, and let K be the number of R peaks as before. Define N by the equation

$$N = \min [N_j], \quad j = 1, \cdots, K - 1$$

where N_j is the number of sample points in complex j.

Then, averaging can be expressed as follows:

$$y_i = \frac{1}{K-1} \sum_{j=1}^{K-1} y_{(M_j+i-1)}$$

where y_i represents the average ECG amplitude at time

$$t = i \quad (i = 1, 2, \cdots, N/2).$$

The second half of the average ECG complex can be obtained as

$$y_L = \frac{1}{K-1} \sum_{j=2}^{K} y_{(M_j+1-N)}$$

where $L = N/2, \cdots, N$.

In this manner, elimination of a number of samples within the inactive region is automatically achieved without having to align the individual heartbeats.

B. Processing: Waveform Detection and Parameter Extractions

1) QRS Detection: The *QRS* detection is achieved by first finding the maximum spatial velocity of an ECG file (see Fig. 1(e) and the Appendix) and then setting a threshold at 60 percent of the maximum value; this method of waveform detection is somewhat similar to that of Stallman and Pipberger [9]. If the spatial velocity at any point in the data record surpasses this threshold, a window is established at 20 and 30 ms before

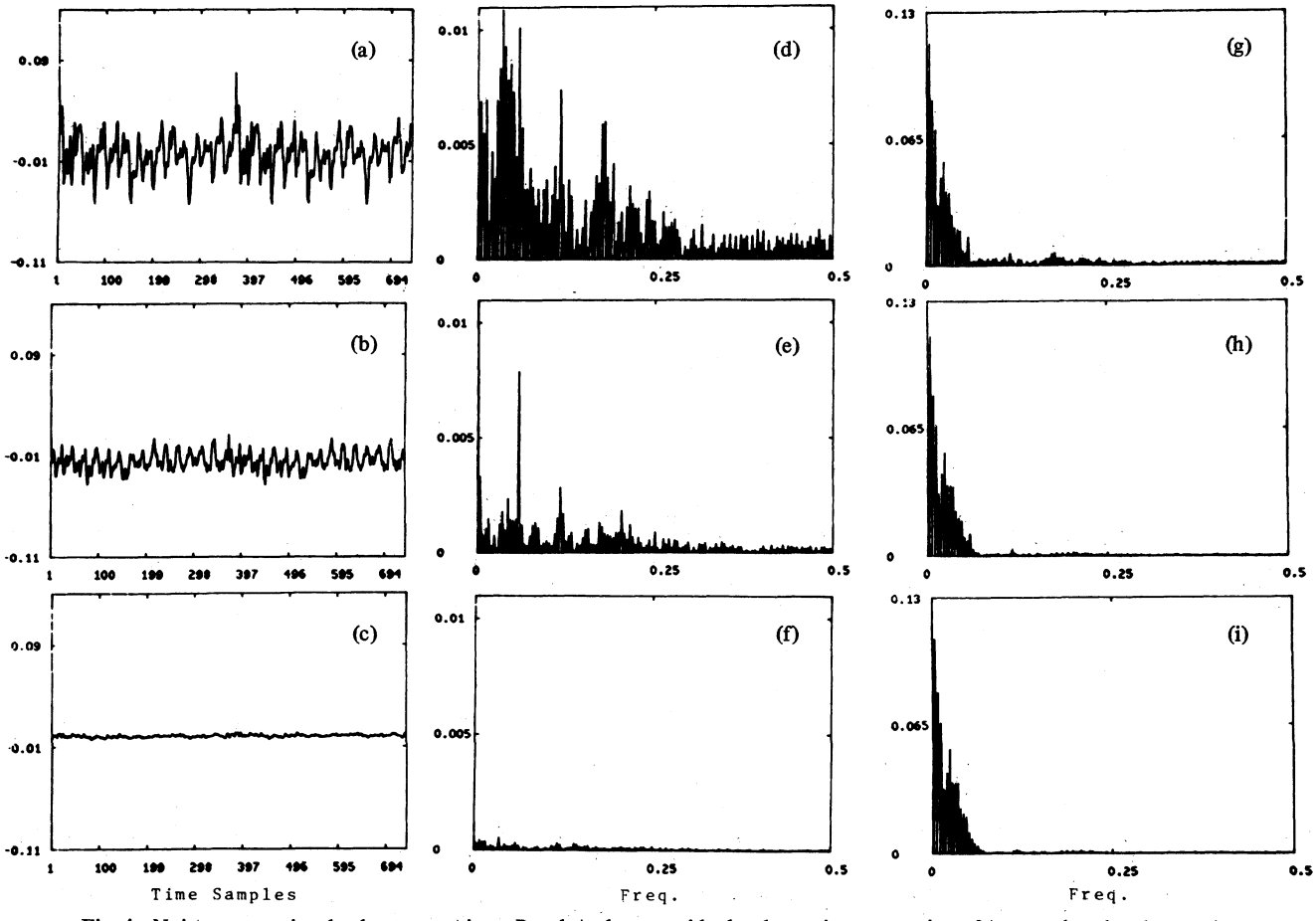

Fig. 4. Noise suppression by beat averaging. Panel A shows residual voltages in raw tracing after template has been subtracted. Panel B shows residual of 7-beat average after template subtraction; panel C, the residual of 13-beat average after template subtraction. The template is a 14-beat average. Panels D, E, and F show the power spectra of data in panels A, B, and C, respectively. Panels G, H, and I show power spectra of raw data, 7-beat average, and the 14-beat average. Note that spectra on the latter panels retain their essential pattern relating to the signal, whereas spectra of residual noise are reduced in middle panels by beat averaging.

and after the threshold. A search is then performed through the spatial magnitude to determine the *R*-wave peak.

2) QRS Onset and QRS Offset: The *QRS* onset is determined by conducting a backward search through a 40 ms window from the *R*-wave peak. The *QRS* onset is flagged as the point where the spatial velocity goes below a threshold of 1.5 mV/s. If the *QRS* onset is not detected within the prescribed time window, the average beat is plotted and execution of the algorithm is halted.

The *QRS* offset is precisely determined from the *R*-wave peak as the point where the spatial velocity goes from negative to positive. This fiducial point is also defined as the beginning of the *T* wave since, in rat ECG's, the *S-T* segment is absent [1].

3) T-Wave Detection: From the *T*-wave beginning (*QRS* offset), a search is performed over a 50 ms window for the peak of the *T* wave. Once the peak is found, the *T*-wave end is searched over a 70 ms window. The *T*-wave end is defined as a point where the spatial velocity goes above a threshold of -0.25 mV/s. If no *T* wave is detected, a flag is set.

4) P-Wave Detection: The *P* wave is detected by defining a slope threshold of 5 mV/s. Once the *P* wave is found, a backward search is conducted over a 20 ms window for the *P*-wave beginning. Then, a forward search is performed from the threshold point for the *P*-wave end.

5) Parameter Extractions: With the *P*, *QRS*, and *T* waves detected, various parameters such as the heart rate, *PR* segment, *P* duration, *QRS* width, and *T* duration are calculated, and a vector loop of the corresponding ECG tracing is constructed on the Calcomp plotter. A sample run of the described algorithm is shown in Figs. 5 and 6.

IV. General Performance

In the design of a system for the automated analysis of rodent ECG's and VCG's, the degree of interindividual variability must be carefully considered. In the case of rodents, there exists a very large range of variability in the ECG's rhythms (200-600 beats/min). Thus, a self-adjusing procedure has been developed to permit a general adaptation of wave-detection algorithms. Furthermore, the automated analysis of rodent ECG's is complicated by the various amounts of interference such as power line interference, random muscle noise, and especially baseline wander which often occurs during the ECG recordings due to body movements.

An approach which Keiser and Meyer [5] developed is found to be very effective in the removal of baseline wander; this procedure uses cubic spline fitted through the *P-R* knots. Since there is usually a substantial overlap of the baseline wander spectrum and the cardiac signal spectrum, the cubic spline

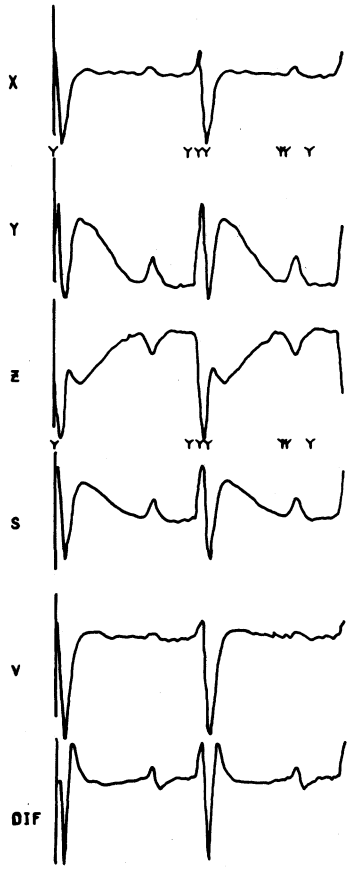

Fig. 5. Plot of the *X*, *Y*, and *Z* lead after averaging. Lead II (standard lead) is also shown. *V*: spatial magnitude; *DIF*: spatial velocity. Markers "*Y*" indicate the *QRS* onset and offset, *T* end, *P* beginning, and *P* end.

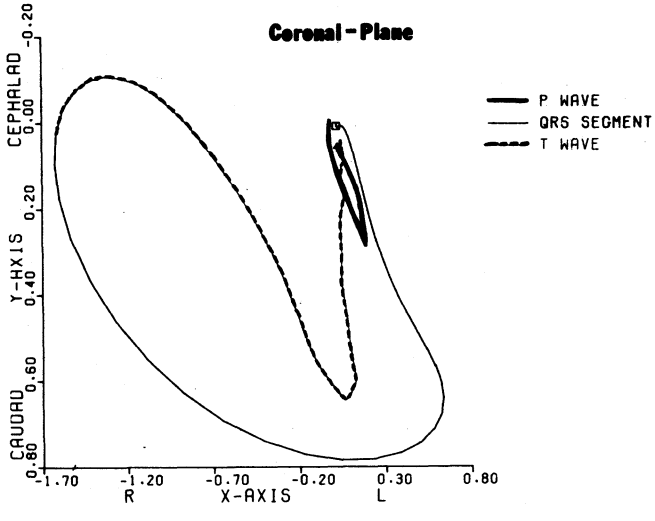

HEART RATE (BEATS/MIN)	435.
QRS-INTERVAL(MSEC)	18.000
PR-INTERVAL(MSEC)	20.800
QT-INTERVAL(MSEC)	89.600
P-DURATION(MSEC)	23.200
T-DURATION(MSEC)	72.000

Fig. 6. Plot of vector loop and printout of timing parameters.

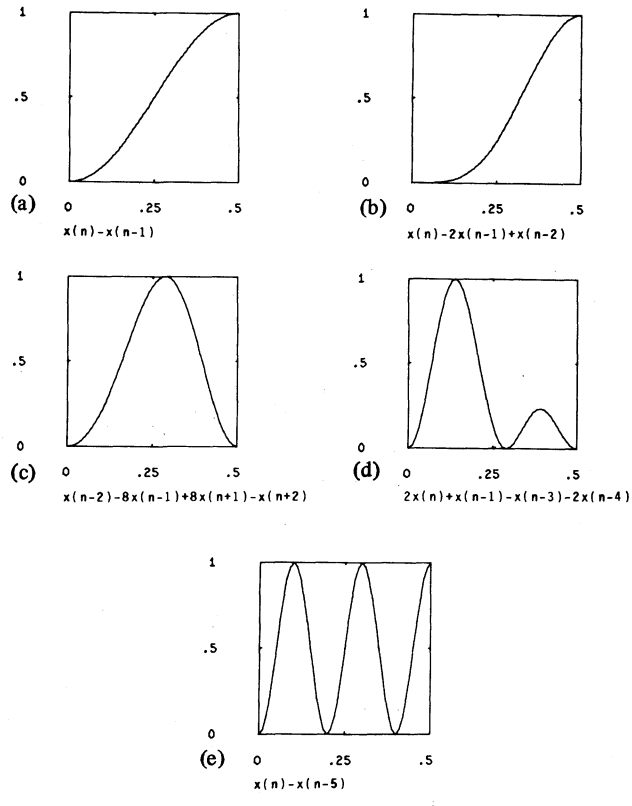

Fig. 7. Spectral sensitivity of slope formulas.

method has provided a reliable procedure to remove baseline drifts while preserving the low-frequency components of the signal. In addition, this process also adjusts for respiratory variations in heart rate by fitting the spline function through a set of *P-R* knots. This, in effect, results in a "self-adjustable" high-pass filter. In 10 percent of the cases, however, sudden baseline shifts due to large muscle spikes are present in the *QRS* complexes, and therefore cannot be removed using the cubic spline method. This condition is treated as an artifact and is deleted from the data set during the averaging process. In addition, if there are long segments of baseline wander with a frequency exceeding one-fourth of the heart rate (0.83-2.5 Hz for 200-600 beats/min ECG record), the cubic spline method will fail. This occurs rarely, but when it does, the ECG is not interpretable visually or automatically.

Shown in Fig. 7(d) is the spectral sensitivity of the implemented slope formula for *QRS* detection. Considering that the slope threshold is set at 60 percent of the maximum *QRS* slope, this implies, for example, that high-frequency noise of 200 Hz must exceed 15 percent of the *QRS* amplitude to trigger a false detection (a signal-to-noise ratio of 7:1). Fig. 8 illustrates a plot of the required noise amplitude as a fraction of the *QRS* amplitude versus the noise frequency in order for a false *QRS* detection to occur. In addition, such a slope formula is also highly insensitive to low-frequency components. Thus, only baseline wander of exceedingly high magnitude can cause a false *QRS* detection.

As shown in Fig. 4, the signal-averaging procedure has provided an efficient means of reducing the total noise power. On the average, this procedure has improved the signal-to-noise ratio by a factor of four (amplitude). One limitation, however, with the averaging method is that it requires a similarity cluster

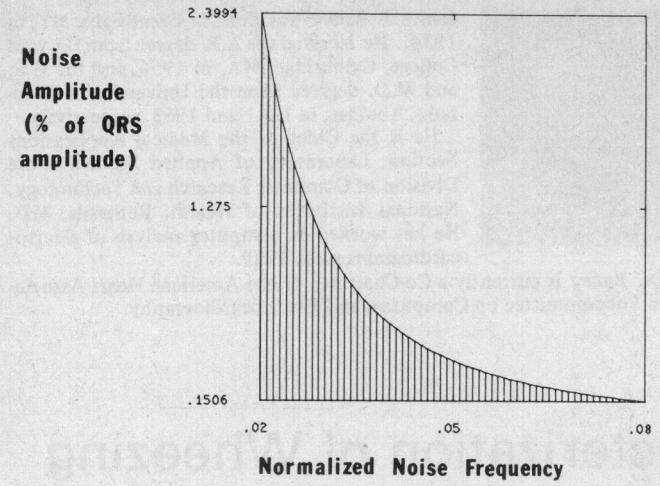

Fig. 8. Plot of noise amplitude as a fraction of *QRS* amplitude versus normalized noise frequency (sampling rate = 2500). Shaded region: region of correct detection.

of *QRS* complexes. In cases where there exist continuous changes in *QRS* morphology (due to changes in conduction paths) or severe arrhythmia, the averaging process fails to construct a reliable *QRS* template. In cases of wandering atrial pacemaker, the template may show a *QRS* pattern without a definable *P* wave.

Thus far, this algorithm has been tested on 50 cases of rat ECG's, and 48 cases or 96 percent were successfully analyzed. Those cases which failed consist of ECG tracings with a very low signal-to-noise ratio.

Appendix

Slope Spectral Sensitivity

The reliability of fiducial determinations depends on accurate *QRS* detections. Thus, it is crucial that an effective algorithm be used to distinguish between high-frequency *QRS* and noise components. Fig. 7 (a)-(e) illustrates the spectral sensitivity of different slope formulas.

While the first difference [Fig. 7(a)] measurement is an effective algorithm for noise-free signal, it is very vulnerable to high-frequency noise. In the ECG algorithm, we use slope formula 7(d) in detecting the *QRS* complexes since it is less susceptible to high-frequency noise as compared to the others. However, once the average beat with a low level of high-frequency noise is formed, the slope formula(s) is used to detect the *P*, *QRS*, and *T* waves.

Shown in Fig. 8 is a plot of the noise as a fraction of the *QRS* amplitude versus normalized frequency. In this illustration, it is assumed that the *QRS* frequency is centered at 100 Hz, and thus has a spectral sensitivity of S_Q given in Fig. 7(d). Considering that the slope threshold is set at 60 percent of the maximum *QRS* amplitude, an approximate region of correct *QRS* detection can be evaluated as follows:

$$E(f_N) < \frac{0.6\, S_Q}{S(f_N)}$$

where $f_N = f/f_s$ is the normalized frequency and $f_s = 2500$ Hz is the sampling rate. The above simplified model and assumptions yield a rough estimate of the overall performance of the *QRS* detector with the presence of high-frequency noise.

References

[1] R. Budden, D. K. Detweiler, and G. Zbinden, *The Rat Electrocardiogram in Pharmacology & Toxicology.* London, England: Pergamon, 1981.
[2] B. E. Osborne, "Uses and applications of electrocardiography in toxicology: Experimental model systems in toxicology and their significance in man," *Excerpta Medica*, vol. 15, pp. 85–97, 1974.
[3] J. J. Spitzer, *Myocardial Injury.* New York: Plenum, 1983.
[4] A. V. Oppenheim and R. W. Schafer, *Digital Signal Processing.* Englewood Cliffs, NJ: Prentice-Hall, 1975.
[5] J. Wartak, *Computers in Electrocardiography.* Chicago, IL: Thomas, 1970.
[6] C. R. Meyer and H. N. Keiser, "Electrocardiogram baseline noise estimation and removal using cubic splines and state-space computation techniques," *Comput. Biomed. Res.*, vol. 10, pp. 459–470, 1977.
[7] L. L. Horowitz, "The effects of spline interpolation on power spectral density," *IEEE Trans. Acoust., Speech, Signal Processing*, vol. ASSP-22, pp. 22–27, Feb. 1974.
[8] H. T. Le, "A system for automated analysis of rodent ECG," M.S. thesis, Dep. Elec. Eng., Univ. Maryland, College Park, 1984.
[9] F. W. Stallmann and H. V. Pipberger, "Automatic recognition of electrocardiographic waves by digital computer," *Circ. Res.*, vol. 9, pp. 1138–1143, 1961.

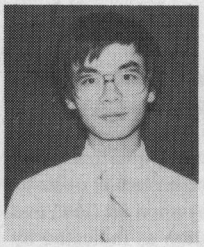

Hung T. Le was born in Saigon, Vietnam, on May 10, 1961. He received the B.S. degree from the University of Virginia, Charlottesville, in 1982, and the M.S. degree from the University of Maryland, College Park, in 1984, both in electrical engineering.

During his graduate studies at the University of Maryland, he held a position at the National Institutes of Health, Bethesda, MD, conducting research in digital signal processing with applications to biomedical problems. He is presently with IBM, Manassas, VA, working in acoustics development for the Submarine Advanced Combat System.

Mr. Le is a member of Tau Beta Pi and Eta Kappa Nu.

William C. Van Arsdel was born in Indianapolis, IN, on April 27, 1920. He received the B.S. degree in pharmacology from the University of Oregon Medical School, Eugene, and the Ph.D. degree in physiology (zoology) from Oregon State University, Corvallis.

He has been a Pharmacologist in the Bureau of Drugs (now the Center for Drugs and Biologics), FDA, Washington, DC, since 1963. His thesis and postdoctoral research at Oregon State involved electrocardiology of large animals (cattle). His current research with the Division of Drug Biology involves the use of laboratory animal indicators of cardiac toxicity and/or injury in drug testing.

Armand M. Makowski (M'82) was born in Watermael-Boitsfort, Belgium, on October 9, 1953. He received the Licence en Sciences Mathematiques from the University Libre de Bruxelles in 1975, the M.S. degree in engineering-systems science from the University of California, Los Angeles, in 1976, and the Ph.D. degree in applied mathematics from the University of Kentucky, Lexington, in 1981.

In August 1981 he joined the Faculty of the Department of Electrical Engineering, University of Maryland, College Park, where he is presently an Assistant Professor. His research interests lie primarily in the areas of stochastic dynamical optimization, statistical signal processing, and more broadly, in the applications of the theory of stochastic processes to engineering problems. More recently, he has been working on problems of adaptive optimal control for queueing systems, and on various applications of nonlinear (stochastic) filtering and digital signal processing.

Dr. Makowski was a C.R.B. Graduate Fellow of the Belgian–American Educational Foundation for the academic year 1975–1976. He is a recipient of the 1984 NSF Presidential Young Investigator Award.

Erik W. Pottala was born in Fitchburg, MA, in 1939. He received the B.S. degree from Worcester Polytechnic Institute, Worcester, MA, in 1961, the Master's of Engineering degree from Yale University, New Haven, CT, in 1963, and the Ph.D. degree from the University of Maryland, College Park, in 1970.

He is an Electronic Engineer with the Medical Applications Section, Laboratory of Applied Studies in the Division of Computer Research and Technology, National Institutes of Health, Bethesda, MD. He is currently engaged in analog-to-digital conversion and physiological modeling.

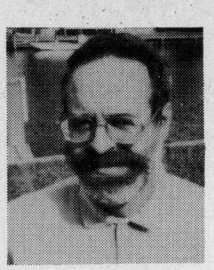

James J. Bailey was born in Great Falls, MT, in 1934. He received the A.B. degree from Harvard College, Cambridge, MA, in 1956, and the M.S. and M.D. degrees from the University of Colorado, Boulder, in 1961 and 1965, respectively.

He is the Chief of the Medical Applications Section, Laboratory of Applied Studies in the Division of Computer Research and Technology, National Institutes of Health, Bethesda, MD. He has worked on computer analysis of electrocardiograms since 1969.

Dr. Bailey is currently a Co-Chairman of the American Heart Association Subcommittee on Computers and Electrocardiography.

Automated Spectral Characterization of Wheezing in Asthmatic Children

T. RICHARD FENTON, MEMBER, IEEE, HANS PASTERKAMP, A. TAL, AND VICTOR CHERNICK

Abstract—**Breath sounds were recorded in normal and asthmatic children over the chest and trachea. The power spectra of the sounds were analyzed for peaks of high amplitude and high frequency as indications of wheezing. The percent of inspiration and expiration spent wheezing was used as an indication of the severity of bronchial obstruction. Wheezing was found to be strongly dependent upon air flow, and generally followed the changes in pulmonary function as indicated by the forced expiratory volume at 1 s (FEV1). The trachea was found to be a better location for analyzing wheezes than the lung.**

I. Introduction

WHEEZES are clinically defined as abnormal, more or less melodic tones of distinguishable pitch which last longer than 100 ms [14]. They have been termed continuous added lung sounds, implying that they are superimposed on normal breath sounds and relatively continuous when compared to other abnormal sounds, such as crackles which typically last 10 ms [16]. When studied with spectral analysis, wheezes are seen as narrow peaks in the power spectrum, generally below 2000 Hz [8].

Wheezing is of very practical importance in the diagnosis and management of a number of pulmonary pathologies, such as asthma and bronchiolitis. The presence and location of the wheeze, its duration, and its relation to the respiratory cycle all assist the physician in his assessment of the patient [8].

Manuscript received January 24, 1984; revised July 15, 1984. This work was supported by the Winnipeg Children's Hospital Research Foundation, Winnipeg, Man., Canada. The work of H. Pasterkamp was supported by the Manitoba Lung Association, Canada. The work of A. Tal was supported by the Faculty Fund, Faculty of Medicine, University of Manitoba, Winnipeg, Man., Canada.

T. R. Fenton is with the Department of Biomedical Engineering, Health Sciences Centre and the Departments of Energy and Electrical Engineering, University of Manitoba, Winnipeg, Man., Canada R3E 0Z3.

H. Pasterkamp and V. Chernick are with the Department of Pediatrics, University of Manitoba, Winnipeg, Man., Canada R3E 0Z3.

A. Tal is with the Department of Pediatrics, University of Manitoba, Winnipeg, Man., Canada, on leave from Ben Gurion University, Beer-Sheva, Israel.

Simple auscultation is not sufficiently objective to permit reliable comparison of wheezing over periods of time nor over different parts of the chest and trachea [20]. So far, few automated methods have been developed to make the detection and characterization of wheezing more reliable and specific, and clinical application of these techniques has been very modest. This is due in part to the complexity of the apparatus and to the awkwardness of the procedure relative to conventional auscultation which has remained essentially unmodified since it was established in 1819 [12].

The most straightforward automated method is to compute the power spectra of random finite record lengths of lung sounds [2], [17]. These spectra are commonly described by their predominant frequency and signal bandwidth [4], [9]. Since air flow is known to determine breath sound intensity [13], it is normally necessary to incorporate additional calculations such as successive averaging into these analyses to achieve reliability. If the patients are cooperative, air flow may be included with the measurements so that the records are taken under more defined and repeatable conditions [4]. In very young children, respiration signals may be derived from thoracic impedance [18].

The present study was designed to develop an objective computer-aided analysis of wheezing in children, and to apply the technique in studying the evolution of asthmatic attacks. Both lung and tracheal sounds were included, as it has been suggested that in some patients tracheal auscultation may be more useful [14].

II. Methods

Protocol

Five asthmatic subjects, ages 10–16 years, were studied during spontaneous or induced asthma attacks, and 20 min after therapeutic relief of bronchial obstruction with 200 μg of inhaled Salbutamol. For induced asthma, three subjects were exercised on a bicycle ergometer for approximately 10 min to

0018-9294/85/0100-0050$01.00 © 1985 IEEE